PROCEEDINGS OF SPIE

SPIEDigitalLibrary.org/conference-proceedings-of-spie

Ultrafast, laser-scanning time-stretch microscopy with visible light

Wenwei Yan
Jianglai Wu
Kenneth K. Y. Wong
Kevin K. Tsia

SPIE.

Ultrafast, laser-scanning time-stretch microscopy with visible light

Wenwei Yan[a], Jianglai Wu[a], Kenneth K. Y. Wong[a], and Kevin K. Tsia[a]

[a]Department of Electrical and Electronic Engineering, The University of Hong Kong, Pokfulam Road, Hong Kong

ABSTRACT

We demonstrate ultrafast time-stretch microscopy in, to the best of our knowledge, the shortest wavelength regimes, i.e. 532 nm. This is enabled by a new all-optical ultrahigh-speed laser-scanning technique called *free-space angular-chirp-enhanced delay* (FACED) that achieves a line-scan rate as high as 20 MHz. In contrast to the predominant fiber-based implementation, time-stretch imaging based on FACED allows wavelength-independent and low-loss operations, and more intriguingly reconfigurable all-optical laser-scanning rate. Using this technique, we present high-resolution single-cell images captured in an ultrafast microfluidic flow (1.5m/s). This could unleash numerous cell and tissue imaging applications, e.g. high-throughput image flow cytometry and whole-slide imaging.

Keywords: Image cytometry, optofluidics, time-stretch imaging, ultrafast laser scanning

1. INTRODUCTION

Laser-scanning microscopy has been the gold standard of high-resolution cellular imaging. It has widely been used in applications such as confocal microscopy and nonlinear optical microscopy. However, the current imaging speed is largely limited by the mechanical inertia involved in the common laser-scanning strategies (e.g. using galvonometric mirrors, resonant mirrors), which generally can deliver a line-scan rate no more than 10's kHz [1]. Yet, it is inadequate to address the widespread need for speed in real-time monitoring of fast dynamical processes and high-throughput screening, in which a line-scan rate above MHz is necessary. Among all available techniques, optical time-stretch microscopy, emerged as an all-optical laser-scanning imaging modality, enables an ultrafast line-scan rate beyond tens of MHz [2,3]. In order to create 1D line scan, traditional time-stretch microscopy relies on a two-step mapping process: spectral-encoding and dispersive Fourier transform, that requires the use of broadband pulsed laser and dispersive media such as optical fibres. Due to fibre transmission loss, previous time-stretch imaging demonstrations were mostly limited to NIR regime, leaving the customary microscopy window, i.e. visible wavelengths, uncharted [2,3]. Compared to NIR light, microscopy at visible wavelength provides not only higher diffraction-limited resolution, but also wider range of imaging modalities due to the availability of higher intrinsic (e.g. Chloroplast) and extrinsic (e.g. hematoxylin and eosin stain, fluorescence labels) contrast. In light of this challenge, here we employ a newly developed all-optical laser scanning imaging technique termed *free-space angular-chirp-enhanced delay* (FACED) [4], which enables ultrafast cellular imaging in the visible-light regime.

2. WORKING PRINCIPLE OF FACED

FACED employs a pair of quasi-parallel mirrors for direct space-time mapping without involving the concept of spectral-encoding (Fig. 1a). Incoming focused beam at the entrance of the FACED device (O) is decomposed into a set of spatially-chirped zig-zag light paths, each of which returns back to the entrance with a different time-delay according to the corresponding path length in the round trip. In fact, the concept can be generalized as effectively generating an array of N virtual sources, each of which is separated from each other in space and has a time delay of τ with the adjacent source. As a result, using the intermediate relay optics and objective lens, these spatiotemporally encoded

Imaging, Manipulation, and Analysis of Biomolecules, Cells, and Tissues XV, edited by Daniel L. Farkas, Dan V. Nicolau, Robert C. Leif, Proc. of SPIE Vol. 10068, 100681C
 · doi: 10.1117/12.2251094

virtual sources are projected and demagnified onto the specimen plane in a form of *all-optical* scanning beam. Their spatial and temporal positions can be flexibly reconfigured by the geometric design, i.e. mirror tilt angle α, incoming cone angle β and mirror separation S [4]. Similar to time-stretch imaging, FACED imaging generates a stretched temporal waveform as the line-scan. However, the waveform actually consists of a train of sub-pulses, each of which is the virtual source (Fig. 1b). Also, no chromatic dispersion nor spectral-encoding is involved in FACED imaging – an important and new attribute enabling ultrafast all-optical laser-scanning imaging at visible light wavelengths without the need for broadband sources.

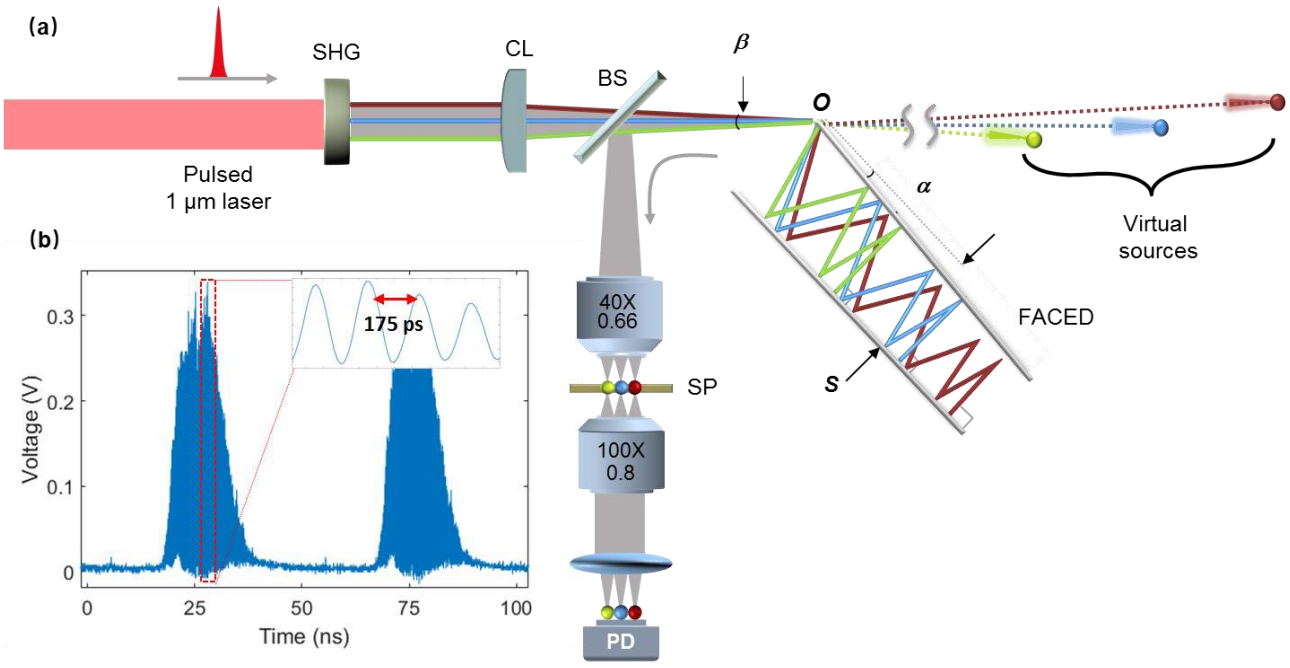

Figure. 1. (a) Schematic of the 532-nm FACED microscope. A picosecond pulsed laser at 1064 nm is first launched through a KTP crystal for second harmonic generation (SHG). A cylindrical lens then focuses the SHG pulsed beam (532 nm) to the FACED device (i.e. the pair of quasi-parallel plane mirrors), which creates ~100 virtual sources with a time delay of ~175 ps between adjacent sources. The spatial-temporally encoded pulsed beam is focused onto a homemade microfluidic channel across a field-of-view of ~40 μm. Finally, a high-speed single-pixel photodiode (10 GHz) captures the spatiotemporally-encoded image signals. CL, cylindrical lens. BS, beam splitter. SP, specimen plane. (b) Waveform of two line scans, each of which consists of ~100 sub-pulses, as shown in the inset. The temporal width of each sub-pulse is determined by both original pulse width as well as the bandwidth of the detection system.

In this work, we demonstrate FACED laser-scanning microscopy at 532 nm for tissue-wide imaging, optofluidic cellular imaging and more importantly the application for image-based single-cell analysis. Specifically, we employ a narrow-band pulsed source (centre wavelength: 532 nm, pulse width:100 ps, bandwidth <0.3 nm) generated through second harmonic generation from a Nd:YVO_4 mode-locked laser through a KTP crystal. Here, the mirror separation S is fixed at ~26 mm, corresponding to a time delay τ of 175 ps between adjacent virtual sources. The input cone angle and tilt angle is optimized to generate ~100 linear-spaced virtual sources, which translates to 100 1D laser scanning points across a 40 μm field-of-view. The line-scan rate of the FACED microscope is determined by the laser repetition rate, which is as high as 20 MHz.

3. RESULTS AND ANALYSIS

We first demonstrate ultrafast laser scanning microscopy for tissue-section and single-cell microfluidic flow imaging. Figures 2a and 2b show the stained cartilage tissue section (methylene blue and fast red) images captured by our FACED

microscope and a conventional transmission bright-field light microscope, respectively. Clearly, the ultrafast FACED laser scanning microscope shows comparable image quality to that in conventional transmission bright-field light microscope (see also the zoomed-in views in Figures 2c and 2d), but at a much higher imaging speed (i.e. 20 MHz line-scan rate). We also examined the single-cell (microphytoplankton) imaging performance under an ultrafast microfluidic flow, ~1.5 m/s. Here, FACED microscopy delivers motion-blur free images of single cells that shows the characteristic subcellular structures, e.g. inner granules and spines of the microphytoplankton.

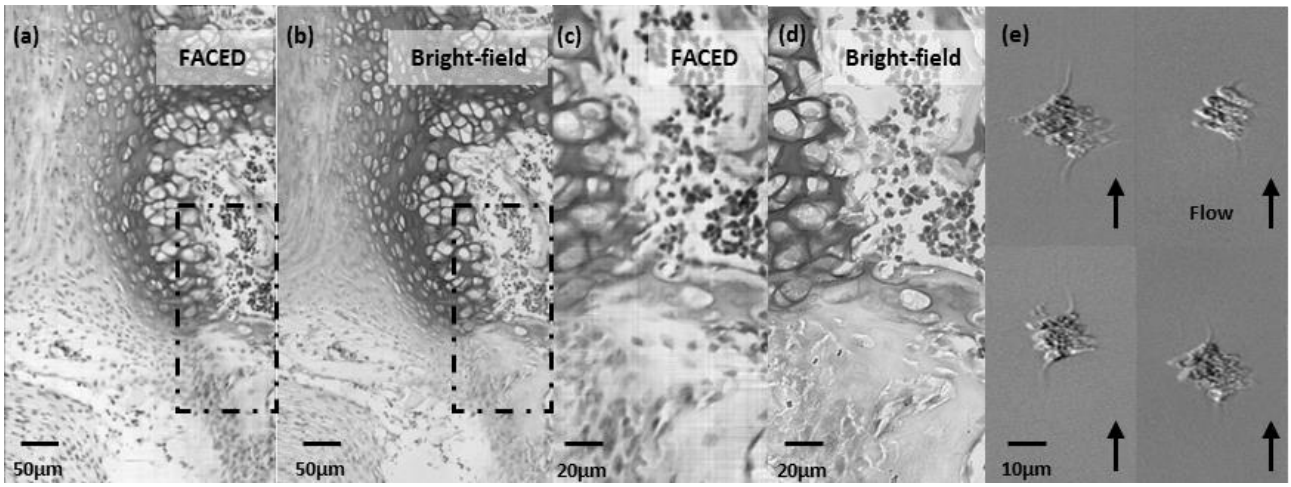

Figure. 2. Basic imaging performance of FACED microscopy (at 532 nm) at a line-scan rate of 20 MHz. (a) Ultrafast laser scanning of vertebral column stained with Alcian blue and nuclear fast red. (b) Bright-field image of the same region for comparison (NA = 0.5). (c-d) Zoomed-in view (Boxed area in a, b) (e) Images of *Scenedesmus acutus* in high-speed microfluidic flow (~1.5 m/s).

Note that the flow speed (1.5m/s) corresponds an imaging throughput of 10,000 – 100,000 cells/sec. Therefore, offering high-resolution as well as high-throughput single-cell imaging, FACED microscopy is particularly valuable for large-scale image-based single cell analysis. To further demonstrate its advantage of visible-wavelength operation (as compared to conventional time-stretch imaging) and thus its compatibility to the common biochemical-specific stains/labels used in cell biology studies, we employ neutral red (Sigma) as a vital stain, which specifically binds to lysosomes, to visualize the morphological changes of human monocytic leukemia cells (THP-1) induced by nutrient starvation under FACED microscopy. At physiological PH, the dye has a net charge close to zero and can passively diffuse across cell membrane. In living cells, the pH difference between the lysosomes and cytoplasm drives the retention of neutral red in lysosomes. In contrast, dead cells could not maintain the pH gradient and therefore fail to retain the stain in the cell [5]. As a result, we could leverage the strong absorbance of neutral red around 500 nm to provide high bright-field contrast change from single-cell images in the present study of nutrient starvation, as shown in Figures 3a and 3b. Comparing to healthy cells, starved cells are clearly characterized in FACED microscopy by their enlarged lysosome compartments with more concentrated neutral red stains. In addition, there is a significant change in cell size. We also implement automated texture analysis of individual cell images using the method of grey level co-occurrence matrix, from which a multitude of single-cell texture parameters can be extracted, such as local spatial homogeneity, contrast and correlation [6]. Here, we exemplify the ability to perform multi-dimensional analysis in terms of optical absorption peak versus its mean value of each cell (Fig. 3c, above) and cell size versus local homogeneity (Fig. 3c, below). Both plots clearly show well separated clusters, corresponding the starved cells and healthy cells, respectively. Note that such capability is absent in conventional neutral red uptake assay in which the analysis is simply based global estimation and fails to report any underlying morphological changes of lysosomes [7]. More importantly, the analysis is based on single-cell images captured at an ultrahigh-throughput beyond 10,000 cells/sec, thanks to the ultrafast line-scan operation in FACED microscopy.

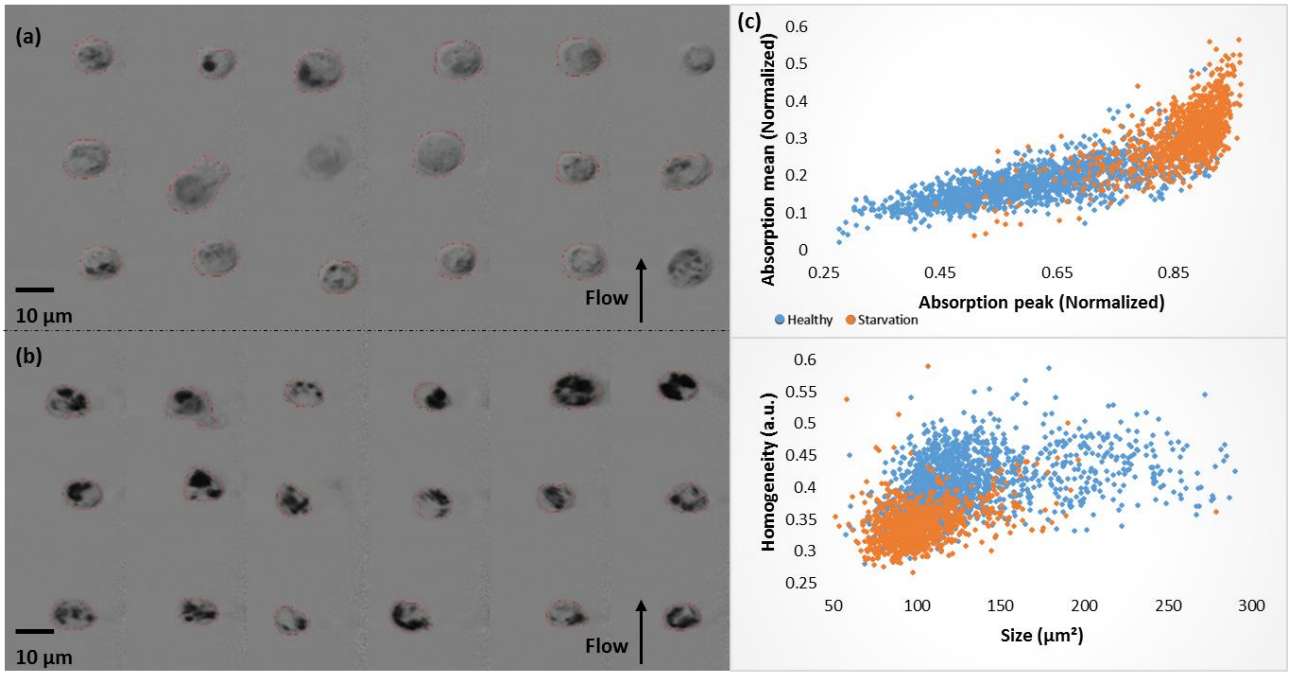

Figure. 3. FACED microscopy of THP-1 (cultured under two different conditions) in the ultrafast microfluidic flow (1.5m/s). THP-1 cells were cultured either in (a) a full (RPMI 1640) or (b) diluted medium (with PBS) for three days. Then, the cells were stained with neutral red, incubated for two hours and followed by FACED microscopy. (c) Selected 2D scatter plots of texture analysis results: (Top) optical absorption mean versus absorption peak of cells, (bottom) local homogeneity and cell size. The computed parameters are derived based on the segmented cell in each image (see the red outlines of the individual cells in (a) and (b)).

4. CONCLUSION

In this work, we present a new modality of all-optical laser scanning microscopy based on free-space angular-chirp-enhanced delay. The advantages include: (I) high throughput cellular imaging with higher image resolution comparing to previous studies, (II) elimination of the dependency on broadband laser and dispersive media and (III) compatibility to biochemical-specific stains commonly used in cell biology. We anticipate that FACED microscopy could be a unique tool for not only high-throughput tissue-wide and single-cell imaging, but also high-speed dynamical imaging if two-dimensional laser-scanning is incorporated. Some future work includes deep, multi-dimensional feature analysis as well as incorporating other imaging modalities such as quantitative phase imaging.

MATERIALS AND METHODS

Microfluidic channel fabrication

The microfluidic channels were fabricated following standard casting technique using polydimethylsiloxane (PDMS) [8]. Firstly, channel design based on the principle of inertial focusing [9] was transferred to a silicon wafer by soft lithography prior to channel fabrication. Then, PDMS was mixed with the corresponding curing agent (10:1) before pouring onto the silicon wafer. PDMS thickness was controlled by spin coating (200 rpm for 1 minute) to achieve a final height of ~0.2 mm. After curing the thin layer of PDMS, a thick, pre-cured PDMS layer with no pattern was physically attached to the inlet/outlet region with un-cured PDMS glue added to strengthen the bonding. The channels were then cured in an incubator at 65 ^{o}C. Afterwards, cured PDMS was demolded and holes were punched for connection to the inlet and outlet. The channel underwent plasma treatment before bonding to a cover slip. Lastly,

plastic tubing was inserted into punched holes inside the thick PDMS layer for fluid transportation with epoxy glue to seal the gap.

THP-1 cell culture

THP-1 cells were cultured in 90% Roswell Park Memorial Institute (RPMI) -1640 medium (Thermo Fisher Scientific, US), 10% fetal bovine serum (FBS) and 1% penicillin-streptomycin (Pen Strep, Thermo Fisher Scientific, US) to reach confluency. Cells were cultured in a CO_2 incubator under 37 ^oC. For nutrient starvation group, cells were harvested and re-suspended in diluted medium (RPMI-1640 with serum added, diluted with 6 times 1x PBS) for three days. Prior to experiment, Neutral red (Sigma-Aldrich) was added to RPMI-1640 with serum to reach the concentration of 40 μg ml^{-1} and incubated overnight in the CO_2 incubator [5]. For each group, cells were harvested and centrifuged to replace original medium with Neutral red medium. After incubation for two hours, neutral red medium was discarded by centrifugation and cells were diluted with 1x PBS before injecting into microfluidic channel.

ACKNOWLEDGEMENT

This work was partially supported by grant from the Research Grants Council of the Hong Kong Special Administrative Region, China (HKU 7172/12E, HKU 720112E, HKU 719813E, HKU 707712P, HKU 17207715, HKU 17205215, HKU 17208414, and HKU 17304514) and University Development Funds of HKU.

REFERENCES

[1] Larson, J. M., Schwartz, S. A. and Davidson, M. W., "Resonant scanning in laser confocal microscopy," (Nikon Microscopy, 2000).
[2] Wong, T. T. W., Lau, A. K. S., Ho, K. K. Y., Tang, M. Y. H., Robles, J. D. F., Wei, X., Chan, A. C. S., Tang, A. H. L., Lam, E. Y., Wong, K. K. Y., Chan, G. C. F., Shum, H. C. and Tsia, K. K., "Asymmetric-detection time-stretch optical microscopy (ATOM) for ultrafast high-contrast cellular imaging in flow," Scientific Reports **4**,3656 (2014).
[3] Goda, K., Ayazi, A., Gossett, D. R., Sadasivam, J., Lonappan, C. K., Sollier, E., Fard, A. M., Hur, S. C., Adam, J., Murray, C., Wang, C., Brackbill, N., Carlo, D. D. and Jalali, B., "High-throughput single microparticle imaging flow analyse," Proc Natl Acad Sci **109**, 11630-11635 (2012).
[4] Wu, J., Xu, Y., Xu, J., Wei, X., Chan, A. C. S., Tang, A. H. L., Lau, A. K. S., Chung, B. M. F., Shum, H. C., Lam, E. Y., Wong, K. K. Y. and Tsia, K. K., "Ultrafast laser-scanning time-stretch imaging at visible wavelengths," Light: Science & Applications **6**, e16196 (2017).
[5] Repetto, G., Peso, A. D. and Zurita, J. L., "Neutral red uptake assay for the estimation of cell viability/cytotoxicity," Nature Protocol **3**, 1125-1131 (2008).
[6] Haralick, R. M., Shanmugam, K. and Dinstein, I. H., "Textural features for image classification," IEEE Trans. Syst. Man Cybern. **3**(6), 610-621 (1973).
[7] Corcelle, E., "Disruption of Autophagy at the maturation step by the carcinogen lindane is associated with the sustained mitogen-activated protein kinase/extracellular signal-regulated kinase activity," Cancer Research **66**, 6861-6870 (2006).
[8] Friend, J. and Yeo, L., "Fabrication of microfluidic devices using polydimethylsiloxane," Biomicrofluidics **4**(2), 026502 (2010).
[9] Oakey, J., Applegate, R. W., Arellano, E., Carlo, D. D., Graves, S. W. and Toner, M., "Particle focusing in staged inertial microfluidic devices for flow cytometry," Analytical Chemistry, **82**(9), 3862-3867 (2010).